MINIMAL CONVEX COMBINATIONS OF SEQUENTIAL LAPLACE-DIRICHLET EIGENVALUES

BRAXTON OSTING AND CHIU-YEN KAO

Abstract. We propose a computational approach based on the level set method to solve shape optimization problems where the objective function is dependent on the Laplace-Dirichlet eigenvalues of the domain. The approach is applied to the parameterized problem of minimizing the convex combination of sequential Laplace-Dirichlet eigenvalues, λ_k and λ_{k+1}. We show that as a function of the combination parameter, the optimal value is non-decreasing, Lipschitz continuous, and concave and that the minimizing set is upper hemicontinuous. The domains which minimize the first few Laplace-Dirichlet eigenvalues are known analytically and/or have been studied computationally and it is known that the optimal solution for some values of k have multiply connected components. Our computations reproduce these previous results for the appropriate parameter values and extend these results, effectively capturing intermediate topology changes. The results are also compared to values obtained analytically for rectangular and elliptical shapes and to values for domains with nearly-circular boundary.

1. Introduction

Since Lord Rayleigh conjectured that the disk should minimize the first Laplace-Dirichlet eigenvalue among all shapes of equal area more than a century ago [42], eigenvalue optimization problems have been an active research topic with applications in various areas including mechanical vibration [17, 16], electromagnetic cavities [1], photonic crystals [18, 19, 28, 21, 39, 38], and population dynamics [27, 43, 24]. Furthermore, eigenvalue optimization problems can be viewed as finding domains (or spatially dependent operator coefficients) which saturate isoperimetric (i.e., universal) inequalities and thus have significant mathematical interest in their own right. Progress has been made on such problems in recent years due to both theoretical and computational developments in optimization methods, variational analysis, and methods for modeling and evolving free interfaces. Excellent surveys on extremum problems for eigenvalues can be found in [22, 4].

In this work, we develop a numerical method for computing optimal domains for shape optimization problems where the objective function is dependent on the Laplace-Dirichlet eigenvalues of the domain, i.e., shape optimization problems of the general form

$$\min_{\Omega\subset\mathbb{R}^d} f(|\Omega|,\Lambda(\Omega)), \tag{1.1}$$

where $\Lambda(\Omega) = \{\lambda_k(\Omega)\}_{k=1}^{\infty}$ are the Laplace-Dirichlet eigenvalues of Ω (see §2 for a mathematical formulation). In our method, the domain is represented using a level set function, which is advantageous when the topology of the optimal domain in (1.1) is unknown. We implement the method in two dimensions ($d = 2$) and use it to study a *parameterized* objective function, where the topology of the optimal domain is known to depend on the parameter. In particular, we consider the γ-parameterized shape optimization problem of minimizing the convex combination of sequential Laplace-Dirichlet eigenvalues

Date: November 1, 2012.

Key words and phrases. shape optimization, Laplacian eigenvalues, Dirichlet boundary condition, isoperimetric problems, and level set methods.

$$\min_{|\Omega|=1} (1-\gamma)\,\lambda_k(\Omega) + \gamma\,\lambda_{k+1}(\Omega), \qquad \text{for } k \in \mathbb{N} \text{ and } \gamma \in [0,1]. \tag{1.2}$$

Our computational results extend and unify several existing results in this area. In what follows, we review some results on eigenvalue optimization problems with an emphasis on computational developments. A summary of this discussion can be found in Table 1.

Related work. It is known that among all open, d-dimensional domains of equal volume, the minimizer of $\lambda_1(\Omega)$ is a ball (Faber-Krahn inequality) and the minimizer of $\lambda_2(\Omega)$ is the union of two balls of equal size (Krahn-Szegö inequality). For $k \geq 3$, considerably less is known about the minimizer of $\lambda_k(\Omega)$. Among quasi-open domains of fixed volume, a minimizer can be shown to exist and have finite perimeter [7, 34], and some connectedness properties are understood [22, 46]. For dimension $d = 2$, it has been conjectured that the two-dimensional, open domain with fixed volume which minimizes $\lambda_3(\Omega)$ is a ball [22]. The minimizer of $\lambda_4(\Omega)$ is conjectured to be the disjoint union of two balls with radii which have ratio $j_{0,1}/j_{1,1}$ where $j_{\cdot,\cdot}$ are zeros of Bessel functions (see [22, open problem 9]. For dimension $d = 2$, candidates for minimizers for $k \leq 15$ have been proposed based on extensive numerical simulations.[1]

Perhaps the first computational contribution to this area was [46], where the range of the first two Laplace-Dirichlet eigenvalues $(\lambda_1(\Omega), \lambda_2(\Omega))$ for a planar domain Ω of unit area was explored. The boundary of the range consists of two rays and a curve connecting their endpoints which was determined numerically by studying the convex combination of the first two eigenvalues. Furthermore, the minimum of $\lambda_j(\Omega)$, for $j = 1:17$ was found when Ω is a union of disjoint circular discs or a union of disjoint rectangles. It was also shown that the minimizing domain is connected for λ_3 and the disc is a local minimum.

In [40], the shape optimization problems of minimizing the first ten Laplace-Dirichlet eigenvalues were studied. A level set approach was used to represent the domain and a relaxed formulation of the Laplace-Dirichlet problem was used to compute the eigenvalues. In [3], the problems of minimizing Laplace-Dirichlet eigenvalues and maximizing Laplace-Neumann eigenvalues were studied. A meshless method was used to compute eigenvalues and eigenfunctions with high accuracy and the boundary of the planar, star-shaped domains were parameterized using Fourier coefficients. The results for the minimal Laplace-Dirichlet eigenvalues were similar to those in [40], except the study was extended to include the eleventh to fifteenth eigenvalues and a significantly improved domain was found for the seventh eigenvalue. The optimal domains are symmetric except for the minimizer for the 13-th Laplace-Dirichlet eigenvalue. This result implies that it is not possible to establish general symmetry properties of extremal domains. For the Laplace-Neumann problem, they found the maximizing domains for the first ten nontrivial eigenvalues.

The related problem of finding the d-dimensional, open domain which maximizes the ratio of the n-th to 1-st Laplace-Dirichlet eigenvalues has also been studied. The maximizer of $\lambda_2(\Omega)/\lambda_1(\Omega)$ was conjectured by Payne, Pólya, and Weinberger to be a ball [41], which was later proven by Ashbaugh and Benguria [5]. In [32], extensive numerical experiments were conducted on various parameterized two-dimensional domains to determine the range of the ratios of the first three Laplace-Dirichlet eigenvalues. A peanut shaped region was found to be a maximizer for the ratio $\lambda_3(\Omega)/\lambda_1(\Omega)$.

In [37], two shape optimization problems were studied: the ratio of the n-th to 1-st Laplace-Dirichlet eigenvalues and the ratio of the n-th eigenvalue gap to 1-st eigenvalue. The eigenvalues were computed using the method of particular solutions and the boundary was parameterized using Fourier-cosine coefficients. A quasi-Newton method was used to improve the convergence of the optimization problem. The optimal values and shapes for $n \leq 13$ are presented. It was found that

[1]Hereafter, when discussing computational results for problems of the form (1.1), the term *minimizer* refers to domains which approximately minimize the discrete version of the objective function. Usage should be clear from context.

Problem	Results
$\min_{\lvert\Omega\rvert=1} \lambda_k$	$k=1$: Minimizer is a ball (Rayleigh-Faber-Krahn), see [22, 4]
	$k=2$: Minimizer is union of 2 balls of equal volume (Krahn-Szegö), see [22, 4]
	$k=3$: Minimizer is connected and a ball is a local minimizer [46]
	$k=4$: Candidate minimizer is union of two balls with different volumes, see [22]
	$k\geq 5$: Numerical results: $k=3:10$ [40] and $k=5:15$ [3]
$\min_{\lvert\Omega\rvert=1} (1-\gamma)\lambda_k+\gamma\lambda_{k+1}$	For $k=1$, only $\gamma=1$ is disconnected [46]
	$k=1$ and $\gamma\in[0,1]$: numerical results [46]
	$k=1:14$ and $\gamma=\frac{1}{2}$: numerical results [2]
	$k=1:5$ and $\gamma\in[0,1]$, (present work)
$\max_{\Omega} \frac{\lambda_k}{\lambda_1}$	$k=2$: Maximizer is a ball (Ashbaugh-Benguria), see [5]
	Numerical results: $k=3$, [32]; $k=3:13$, [37]; $k=3:14$, [2]

TABLE 1. A summary of results for extremizers of functions of Laplace-Dirichlet eigenvalues. See §1.

for both spectral functions and each n, the n-th eigenvalue of the optimal shape has multiplicity of at least two.

In [2], the mean of sequential eigenvalues and ratios of Laplace-Dirichlet eigenvalues are studied. Some results regarding the connectedness of the domains are also derived. The eigenvalues are computed using a meshless method and the regions are parameterized using a Fourier series.

Other ratios, sums, and sums of inverses of Laplace-Dirichlet and Laplace-Neumann eigenvalues have also been studied; see [22, 4]. Recently, a numerical approach based on a B-spline parametrization of the domain boundary was used to study eigenvalue optimization problems [33].

By studying convex combinations of Laplace-Dirichlet eigenvalues, the present work both supports and extends several of these previous results. Additionally, considering the dependence of the optimal solution to (1.2) as a function of the parameter γ reveals an interesting shape evolution for which we can prove several results.

Outline. This paper is organized as follows. In §2, we review the definition and some properties of Laplace-Dirichlet eigenvalues and give some analytical results for the shape optimization problems (1.1) and (1.2). In §3, we consider (1.2) for domains consisting of rectangles and ellipses, where the problem greatly simplifies. These results are used for comparison in subsequent sections. In §4, a robust computational method is introduced for solving problems of the form (1.1). In §5, we apply the computational method to study the convex combination of sequential Laplace-Dirichlet eigenvalues (1.2). Finally, we conclude in §6 with a discussion of results and some further directions.

2. Mathematical preliminaries and formulation

2.1. **Properties of Laplace-Dirichlet eigenvalues.** General references for Laplace-Dirichlet eigenvalues can be found in [15, 22, 29]. In this paper we generally assume $\Omega\subset\mathbb{R}^d$ to be an open, bounded domain with Lipschitz boundary $\Gamma:=\partial\Omega$. Let $\{(\lambda_k(\Omega),\psi_k(\mathbf{x};\Omega)\}_{k=1}^{\infty}$ denote the eigenpairs of the Laplace-Dirichlet operator for the domain Ω (listed with multiplicity), satisfying

$$\begin{aligned} -\Delta\psi(\mathbf{x}) &= \lambda\psi(\mathbf{x}) \qquad \mathbf{x}\in\Omega, \\ \psi(\mathbf{x}) &= 0 \qquad \mathbf{x}\in\Gamma:=\partial\Omega. \end{aligned} \tag{2.1}$$

The eigenvalues $\lambda_k(\Omega)$ are characterized by the Courant-Fischer formulation

$$\lambda_k(\Omega) = \min_{\substack{E_k\subset H_0^1(\Omega)\\ \text{subspace of dim } k}} \max_{\psi\in E_k,\psi\neq 0} \frac{\int_\Omega |\nabla\psi|^2 d\Omega}{\int_\Omega \psi^2 d\Omega} \tag{2.2}$$

where E_k is in general a k-dimensional subspace of $H^1(\Omega)$ and at the minimizer, $E_k = \text{span}(\{\psi_j(\mathbf{x};\Omega)\}_{j=1}^k)$. The ratio in 2.2 is referred to as the Rayleigh quotient. We denote the set of all eigenvalues of a domain Ω by $\Lambda(\Omega) = \{\lambda_k(\Omega)\}_{k=1}^\infty$. The eigenpairs satisfy the following properties:

(1) For fixed Ω, $\lambda_k(\Omega) \uparrow \infty$ as $k \uparrow \infty$.
(2) The eigenvalues are invariant to rigid transformations of the domain, i.e., rotations and translations.
(3) Eigenvalues $\lambda_k(\Omega)$ are monotone with respect to Ω, i.e., $\Omega \subseteq \Omega' \Rightarrow \lambda_k(\Omega') \leq \lambda_k(\Omega)$.
(4) For any $\Omega \subset \mathbb{R}^d$ and $t > 0$, we define $t\Omega := \{t\mathbf{x} \colon \mathbf{x} \in \Omega \subset \mathbb{R}^d\}$. The Laplace-Dirichlet eigenvalues satisfy the homothety property

$$\lambda_k(t\Omega) = t^{-2}\lambda_k(\Omega), \tag{2.3}$$

and thus the quantity $|\Omega|^{\frac{2}{d}}\lambda(\Omega)$ is invariant to dilations of Ω.
(5) If Ω is the disjoint union of two domains, $\Omega = \Omega_1 \cup \Omega_2$, then $\Lambda(\Omega) = \Lambda(\Omega_1) \cup \Lambda(\Omega_2)$.
(6) Let $D \subset \mathbb{R}^2$ be a fixed compact set and $\Omega_j \subset D$ a sequence of open, simply-connected domains which converge in the Hausdorff distance to $\Omega \subset D$. Then $\lambda_k(\Omega_j) \to \lambda_k(\Omega)$. Furthermore, if $\Omega_j \subset \mathbb{R}^2$, $j = 1, 2$ are two star-shaped domains defined by two positive polar functions f_j, i.e., $\Omega_j = \{(r,\theta) \colon r < f_j(\theta),\, \theta \in [0, 2\pi]\}$, then

$$|\lambda_k(\Omega_1) - \lambda_k(\Omega_2)| \leq C\|f_1 - f_2\|_{L^\infty([0,2\pi])}$$

where C is a constant.
(7) If $\partial\Omega$ is Lipschitz, then $\psi \in H^1(\Omega) \cap C(\overline{\Omega}) \cap C^\infty(\Omega)$.
(8) The eigenspace corresponding to $\lambda_1(\Omega)$ is one-dimensional and the eigenfunction $\psi_1(\mathbf{x};\Omega)$ does not change sign on Ω.

2.2. **Shape optimization for Laplace-Dirichlet eigenvalue problems.** In this paper, we study shape optimization problems of the general form (1.1). Recent results show that if $J(\Lambda(\Omega))$ is a non-decreasing and Lipschitz continuous function of the eigenvalues, then a minimizer exists among quasi-open domains of fixed volume and every solution has finite perimeter [7, 34]. For a parameterized optimization function, as in (1.2), the optimal value and minimizing set, when viewed as a function of the parameter, inherit some continuity properties from the objective function. We make these statements precise for (1.2). Recall that a set valued function $\Gamma \colon A \to B$ is *upper hemicontinuous* at a point $a \in A$ if for all sequences $\{a_n\}_n$ such that $a_n \to a$ and all sequences $\{b_n\}_n$ such that $b_n \in \Gamma(a_n)$, there exists a $b \in \Gamma(a)$ such that $b_n \to b$.

Proposition 1. *For the admissible set, $\mathcal{A} := \{\Omega \colon \Omega$ quasi-open and $|\Omega| \leq 1\}$, and objective function, $C_{k,\gamma}(\Omega) := (1-\gamma)\,\lambda_k(\Omega) + \gamma\,\lambda_{k+1}(\Omega)$, define*

$$C^\star_{k,\gamma} = \inf_{\Omega\in\mathcal{A}} C_{k,\gamma}(\Omega) \quad \text{and} \quad \hat{\Omega}_{k,\gamma} = \left\{\Omega \in \mathcal{A} \colon C_{k,\gamma}(\Omega) = C^\star_{k,\gamma}\right\}.$$

For each $k \in \mathbb{N}$ the following statements hold:

(1) For each $\gamma \in [0,1]$, $C^\star_{k,\gamma}$ exists and $\hat{\Omega}_{k,\gamma}$ is a non-empty and closed set. Furthermore, every $\Omega \in \hat{\Omega}_{k,\gamma}$ has finite perimeter.
(2) The optimal value, $C^\star_{k,\gamma}$, is a non-decreasing, Lipschitz continuous, and concave function of γ.
(3) As a set-valued function of γ, $\hat{\Omega}_{k,\gamma}$ is upper hemicontinuous.

Proof. (1) Follows from the results of [7, 34].

(2) Let $0 \leq \beta < \alpha \leq 1$ and let $\Omega_\alpha \in \hat{\Omega}_{k,\alpha}$. Assume $C^\star_{k,\beta} > C^\star_{k,\alpha}$. Then $C^\star_{k,\beta} > C_{k,\alpha}(\Omega_\alpha) \geq C_{k,\beta}(\Omega_\alpha)$ since $C_{k,\gamma}$ is non-decreasing in γ. But this contradicts the optimality of $C^\star_{k,\beta}$. Thus, $C^\star_{k,\gamma}$ is non-decreasing in γ. We compute

$$C^\star_{k,\beta} \leq C_{k,\beta}(\Omega_\alpha) = C^\star_{k,\alpha} + (\beta - \alpha)\left[\lambda_{k+1}(\Omega_\alpha) - \lambda_k(\Omega_\alpha)\right],$$

which shows that $C^\star_{k,\gamma}$ is Lipschitz continuous with constant $\lambda_{k+1}(\Omega_\alpha) - \lambda_k(\Omega_\alpha)$. Let $\gamma_\alpha = (1-\alpha)\gamma_1 + \alpha\gamma_2$ for $\alpha \in (0,1)$ and note that for any Ω, $C_{k,\gamma_\alpha}(\Omega) = (1-\alpha)C_{k,\gamma_1}(\Omega) + \alpha C_{k,\gamma_2}(\Omega)$. Let $\Omega_\alpha \in \hat{\Omega}_{k,\gamma_\alpha}$, i.e., $C_{k,\gamma_\alpha}(\Omega_\alpha) = C^\star_{k,\gamma_\alpha}$ and suppose $C^\star_{k,\gamma_\alpha} < (1-\alpha)C^\star_{k,\gamma_1} + \alpha C^\star_{k,\gamma_2}$. Then

$$\begin{aligned} C_{k,\gamma_2}(\Omega_\alpha) &= \frac{1}{\alpha}C_{k,\gamma_\alpha}(\Omega_\alpha) - \frac{1-\alpha}{\alpha}C_{k,\gamma_1}(\Omega_\alpha) \\ &\le \frac{1}{\alpha}C_{k,\gamma_\alpha}(\Omega_\alpha) - \frac{1-\alpha}{\alpha}C^\star_{k,\gamma_1} \\ &< \frac{1-\alpha}{\alpha}C^\star_{k,\gamma_1} + C^\star_{k,\gamma_2} - \frac{1-\alpha}{\alpha}C^\star_{k,\gamma_1} \\ &= C^\star_{k,\gamma_2} \end{aligned}$$

which contradicts the optimality of $C^\star_{k,\gamma_2}$. This shows that $C^\star_{k,\gamma}$ is a concave function of γ.

(3) Let $M > 0$ be such that $\operatorname{diam}(\Omega) \le M$ for all $\Omega \in \hat{\Omega}_{k,\gamma}$, $\gamma \in [0,1]$. Let $\gamma_n \to \gamma$ and $\Omega_n \in \hat{\Omega}_{k,\gamma_n}$ be sequences. Since the diameter of Ω_n is uniformly bounded, there exists a domain $\Omega \in \mathcal{A}$ and a subsequence (which we denote by Ω_n) such that $\Omega_n \to \Omega$ in the sense of weak γ-convergence [8]. Suppose $\Omega \notin \hat{\Omega}_{k,\gamma}$, i.e., there exists Ω' such that $C_{k,\gamma}(\Omega') < C_{k,\gamma}(\Omega)$. Using the continuity of $C_{k,\gamma}(\Omega)$ in γ and Ω, we compute $\lim_{n\uparrow\infty} C_{k,\gamma_n}(\Omega') = C_{k,\gamma}(\Omega') < C_{k,\gamma}(\Omega) = \lim_{n\uparrow\infty} C_{k,\gamma_n}(\Omega_n)$. For sufficiently large n, this implies $C_{k,\gamma_n}(\Omega') < C_{k,\gamma_n}(\Omega_n)$, contradicting the optimality of Ω_n. Thus, $\hat{\Omega}_{k,\gamma}$ is upper hemicontinuous in γ. □

Using the homothety property of Laplace-Dirichlet eigenvalues (2.3), (1.2) is equivalent to the problem

$$\min_{\Omega\subset\mathbb{R}^d} C_{k,\gamma}(\Omega) := (1-\gamma)\,|\Omega|^{\frac{2}{d}}\,\lambda_k(\Omega) + \gamma\,|\Omega|^{\frac{2}{d}}\,\lambda_{k+1}(\Omega) \tag{2.4}$$

which is of the form (1.1). Computationally, it is more convenient to consider this unconstrained problem, rather than (1.2).

2.3. **Shape deformations.** Gradient-based optimization methods for the solution of (1.1) require the variation of $J(|\Omega|, \Lambda(\Omega))$ with respect to a deformation of the domain Ω, as given in the following proposition.

Proposition 2. *Let $J = J(|\Omega|, \Lambda(\Omega))$ and Ω be a domain for which all eigenvalues λ_k for which J has nontrivial dependence are simple. Then the variation of $J(|\Omega|, \Lambda(\Omega))$ with respect to a deformation of the domain Ω by a velocity field $\mathbf{V}$ is given by*

$$\begin{aligned} \delta J(|\Omega|, \Lambda(\Omega))\cdot\mathbf{V} &= \frac{\partial J}{\partial|\Omega|}\delta|\Omega|\cdot\mathbf{V} + \sum_{k=1}^{\infty}\frac{\partial J}{\partial\lambda_k}\delta\lambda_k(\Omega)\cdot\mathbf{V} \\ &= \left\langle \frac{\partial J}{\partial|\Omega|} - \sum_{k=1}^{\infty}\frac{\partial J}{\partial\lambda_k}|\partial_n\psi_k|^2, V_n\right\rangle_{L^2(\Gamma)} \end{aligned}$$

where $V_n = (\mathbf{V}\cdot\hat{\mathbf{n}})$, $\partial_n = \hat{\mathbf{n}}\cdot\nabla$, $\hat{\mathbf{n}}$ is the outward unit normal, and the eigenfunctions are assumed to be normalized, $\|\psi_k\|_{L^2(\Omega)} = 1$.

Proof. Let $\lambda(\Omega)$ be a simple Laplace-Dirichlet eigenvalue satisfying (2.1) with corresponding eigenfunction ψ. Hadamard's eigenvalue variation formula [22, 23, 20] states that the variation of $\lambda(\Omega)$ with respect to a deformation of the domain Ω by a velocity field $\mathbf{V}$ is given by

$$\delta\lambda(\Omega)\cdot\mathbf{V} = \frac{-\int_\Gamma |\partial_n\psi|^2(\mathbf{V}\cdot\hat{\mathbf{n}})d\Gamma}{\int_\Omega \psi^2 d\Omega}.$$

Noting that $\delta|\Omega|\cdot\mathbf{V} = \int_\Gamma (\mathbf{V}\cdot\hat{\mathbf{n}})d\Gamma$, the result follows from the chain rule. □

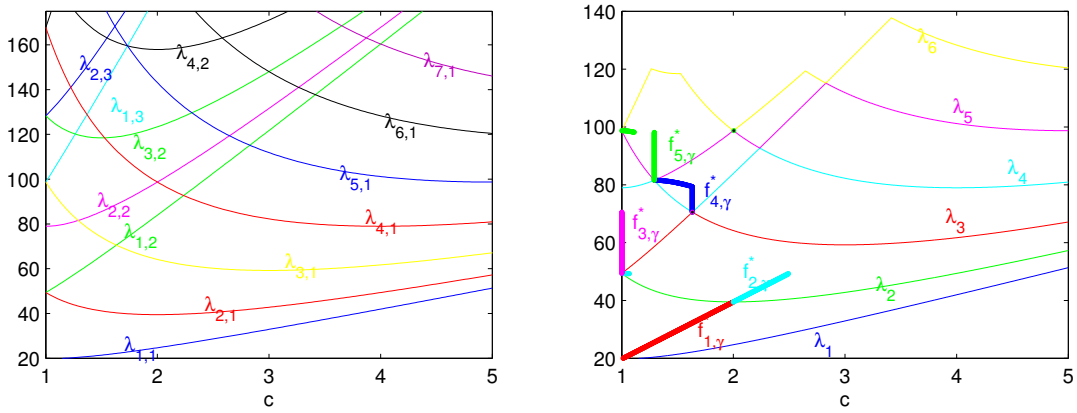

FIGURE 3.1. (left) Eigenvalues λ_{mn} for the rectangular domain $R_c := [0, \sqrt{c}] \times [0, \frac{1}{\sqrt{c}}]$ for $c > 1$ as defined in (3.1). (right) Eigenvalues $\lambda_1 : \lambda_6$ for the rectangular domain R_c for $c > 1$ relabeled by magnitude. Also plotted are the optimal values $f_{k,\gamma}$ for $k = 1 : 5$ and $\gamma \in [0, 1]$. See §3.1.

The following proposition gives the variation of $C_{k,\gamma}(\Omega)$, as defined in (2.4), with respect to a deformation in the domain Ω in two dimensions, i.e. $d = 2$.

Proposition 3. *The variation of* $C_{k,\gamma}(\Omega) := (1-\gamma)\,|\Omega|\ \lambda_k(\Omega) + \gamma\,|\Omega|\ \lambda_{k+1}(\Omega)$ *with respect to a perturbation in the domain* Ω *by a velocity field* $\mathbf{V}$ *is given by*

$$\delta C_{k,\gamma}(\Omega)\cdot\mathbf{V} = \left[(1-\gamma)\lambda_k + \gamma\lambda_{k+1}\right]\delta|\Omega|\cdot\mathbf{V} \ + \ |\Omega|\left[(1-\gamma)\delta\lambda_k(\Omega)\cdot\mathbf{V} \ + \ \gamma\delta\lambda_{k+1}(\Omega)\cdot\mathbf{V}\right]$$

where $\delta|\Omega|\cdot\mathbf{V} = \int_\Gamma (\mathbf{V}\cdot\hat{\mathbf{n}})d\Gamma$.

3. Convex combinations of sequential eigenvalues for two parameterized domains

In this section, we study the convex combination of sequential Laplace-Dirichlet eigenvalues over two classes of one-parameter domains: rectangles and ellipses of fixed area. In both cases, the shape optimization problem (1.2) greatly simplifies. The results obtained are used for comparison in §5.

3.1. Convex combinations of sequential eigenvalues for rectangles.

Consider the one-parameter family of unit-area rectangular domains R_c with length $\sqrt{c}$ and width $\frac{1}{\sqrt{c}}$. Without loss of generality, we assume the aspect ratio c of the rectangle R_c is greater than one, i.e., $c > 1$. The Laplace-Dirichlet eigenvalues of the rectangle R_c are given by

$$\lambda_{m,n} = \pi^2\left(\frac{m^2}{c} + cn^2\right), \quad m, n = 1, 2, 3, 4, \ldots. \tag{3.1}$$

In Fig. 3.1(left), we plot the eigenvalues $\lambda_{m,n}$ for rectangles R_c with varying aspect ratio, c. We relabel the eigenvalues λ_k according to their magnitude, i.e., $0 < \lambda_1 < \lambda_2 \leq \lambda_3 \leq \ldots$. The relabeled eigenvalues are plotted in Fig. 3.1(right). The first six eigenvalues may be expressed:

$$\lambda_1 = \lambda_{1,1} = \pi^2\left(\tfrac{1}{c} + c\right) \qquad \lambda_2 = \lambda_{2,1} = \pi^2\left(\tfrac{4}{c} + c\right)$$

$$\lambda_3 = \begin{cases} \lambda_{1,2} = \pi^2\left(\tfrac{1}{c} + 4c\right), & c \le \sqrt{\tfrac{8}{3}} \\ \lambda_{3,1} = \pi^2\left(\tfrac{9}{c} + c\right), & c \ge \sqrt{\tfrac{8}{3}} \end{cases}$$

$$\lambda_4 = \begin{cases} \lambda_{2,2} = \pi^2\left(\tfrac{4}{c} + 4c\right), & c \le \sqrt{\tfrac{5}{3}} \\ \lambda_{3,1} = \pi^2\left(\tfrac{9}{c} + c\right), & \sqrt{\tfrac{5}{3}} \le c \le \sqrt{\tfrac{8}{3}} \\ \lambda_{1,2} = \pi^2\left(\tfrac{1}{c} + 4c\right), & \sqrt{\tfrac{8}{3}} \le c \le \sqrt{5} \\ \lambda_{4,1} = \pi^2\left(\tfrac{16}{c} + c\right), & c \ge \sqrt{5} \end{cases}$$

$$\lambda_5 = \begin{cases} \lambda_{3,1} = \pi^2\left(\tfrac{9}{c} + c\right), & c \le \sqrt{\tfrac{5}{3}} \\ \lambda_{2,2} = \pi^2\left(\tfrac{4}{c} + 4c\right), & \sqrt{\tfrac{5}{3}} \le c \le 2 \\ \lambda_{4,1} = \pi^2\left(\tfrac{16}{c} + c\right), & 2 \le c \le \sqrt{5} \\ \lambda_{1,2} = \pi^2\left(\tfrac{1}{c} + 4c\right), & \sqrt{5} \le c \le 2\sqrt{2} \\ \lambda_{5,1} = \pi^2\left(\tfrac{25}{c} + c\right), & c \ge 2\sqrt{2} \end{cases}$$

$$\lambda_6 = \begin{cases} \lambda_{1,3} = \pi^2\left(\tfrac{1}{c} + 9c\right), & c \le \sqrt{\tfrac{8}{5}} \\ \lambda_{3,2} = \pi^2\left(\tfrac{9}{c} + 4c\right), & \sqrt{\tfrac{8}{5}} \le c \le \sqrt{\tfrac{7}{3}} \\ \lambda_{4,1} = \pi^2\left(\tfrac{16}{c} + c\right), & \sqrt{\tfrac{7}{3}} \le c \le 2 \\ \lambda_{2,2} = \pi^2\left(\tfrac{4}{c} + 4c\right), & 2 \le c \le \sqrt{7} \\ \lambda_{5,1} = \pi^2\left(\tfrac{25}{c} + c\right), & \sqrt{7} \le c \le 2\sqrt{2} \\ \lambda_{1,2} = \pi^2\left(\tfrac{1}{c} + 4c\right), & 2\sqrt{2} \le c \le \sqrt{\tfrac{35}{3}} \\ \lambda_{6,1} = \pi^2\left(\tfrac{36}{c} + c\right), & c \ge \sqrt{\tfrac{35}{3}} \end{cases}$$

Similar expressions may be obtained for larger eigenvalues λ_k, however, as can be seen from Figure 3.1(right), the number of maximal intervals for which λ_k is smooth increases with k.

For $\gamma \in [0,1]$, define the minimal convex combination of sequential eigenvalues λ_k and λ_{k+1} over the set of all c-parameterized rectangles, i.e., $\{R_c \colon c \ge 1\}$, by

$$c^\star_{k,\gamma} = \arg\min_{c\ge 1} f_{k,\gamma}(c) := (1-\gamma)\,\lambda_k(R_c) + \gamma\,\lambda_{k+1}(R_c) \quad \text{and} \quad f^\star_{k,\gamma} = f(c^\star_{k,\gamma}). \tag{3.2}$$

For example,

$$f_{1,\gamma}(c) = (1-\gamma)\lambda_1(R_c) + \gamma\lambda_2(R_c) = \pi^2\left(c + \frac{1}{c}\,(1+3\gamma)\right).$$

Thus $f_{1,\gamma}(c)$ reaches a minimum for $c^*_{1,\gamma} = \sqrt{1+3\gamma}$ with value $f^\star_{k,\gamma} = 2\pi^2\sqrt{1+3\gamma}$. The minimizing sets $c^\star_{k,\gamma}$ and minimal values $f^\star_{k,\gamma}$ for $k = 1:5$ are presented in Table 2 and Figure 3.2. The numerical values of $f^\star_{k,\gamma}$ for $k = 1:5$ and $\gamma = 0:.1:1$ are given in Table 3(top). We observe the following:

(1) For each $k \in \mathbb{N}$ and $\gamma \in [0,1]$, a minimizer of $f_{k,\gamma}(c)$, as defined in (3.2), exists, but is not necessarily unique. Uniqueness can fail at a single point such as for $k = 2$ at $\gamma = \frac{4}{9}$ or over an interval such as for $k = 5$ and $\gamma = [\frac{1}{2}, 1]$.
(2) An argument similar to that for Prop. 1 shows that as a function of the parameter γ, the minimal objective function value $f^\star_{k,\gamma}$ is non-decreasing, Lipschitz continuous, and concave and that the minimizing set $c^\star_{k,\gamma}$ is upper hemicontinuous. From the form of the optimizers in Table 2, one may additionally verify that the minimum $f^\star_{k,\gamma}$ is a piecewise smooth function of γ.
(3) For fixed $k \in \mathbb{N}$, if the optimal value $f^\star_{k,\gamma}$ is constant on the interval $[1-\delta, 1]$ for some $\delta > 0$, then $\lambda_{k+1}(R_{c^\star_{k,1}}) = \lambda_k(R_{c^\star_{k,1}})$, i.e., the multiplicity of $\lambda_{k+1}(R_{c^\star_{k,1}})$ is greater than one. This is observed for $k = 2:5$.

3.2. **Convex combinations of sequential eigenvalues for ellipses.** Any ellipse can be represented in Cartesian coordinates as the set of points $(x,y) \in \mathbb{R}^2$ such that

$$\frac{x^2}{\alpha^2} + \frac{y^2}{\beta^2} \le 1 \qquad \text{where } \alpha > \beta > 0.$$

Here, α and β are referred to as the major and minor radii respectively. The foci of the ellipse are $x = \pm c = \pm\sqrt{\alpha^2 - \beta^2}$, the eccentricity is $\epsilon = \frac{c}{\alpha}$, and the area is $A = \pi\alpha\beta$. For fixed area, the set

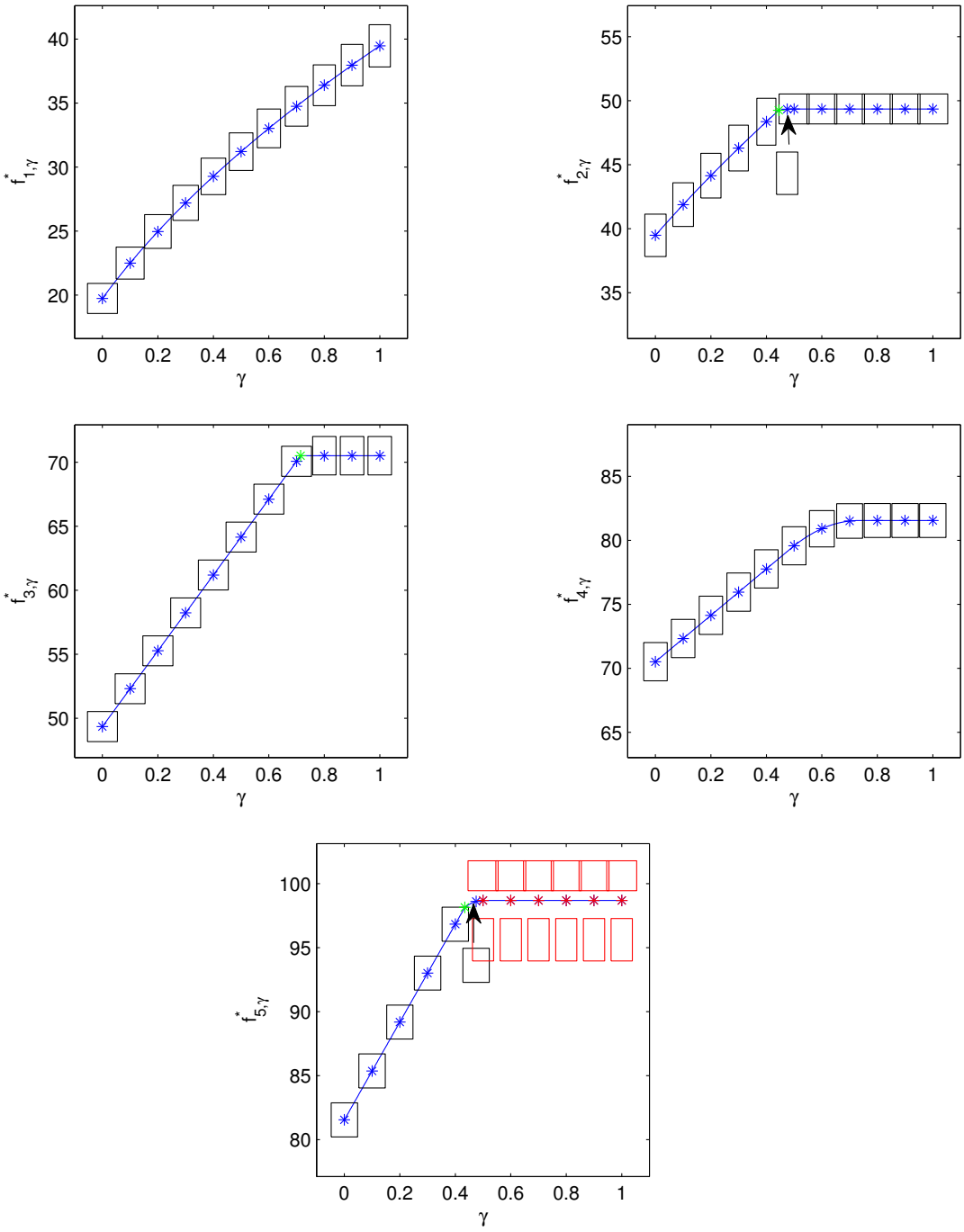

FIGURE 3.2. The optimal values $f^\star_{k,\gamma}$ for $k = 1:5$ and $\gamma \in [0,1]$ as defined in (3.2) are plotted in blue. For each point indicated with an asterisk, the corresponding optimizing rectangle is also presented. For $k = 2$ and 5, additional rectangles are given so that each solution interval in Table 2 is represented. Isolated values γ such that the optimizer is not unique are indicated by the green asterisks ($k = 2$, $\gamma = \frac{4}{9}$; $k = 3$ at $\gamma = \frac{35}{6\sqrt{6}} - \frac{5}{3}$; and $k = 5$,$\gamma = \frac{2\sqrt{15}\sqrt{1769}}{4065} + \frac{96}{271}$). For $k = 5$ the solution is not unique on the interval $\gamma = [\frac{1}{2}, 1]$. Here minimal values are indicated by red asterisks and both minimizing rectangles are presented in red. See Table 2 and §3.1.

k	γ	$c^\star_{k,\gamma}$	$f^\star_{k,\gamma}$	Mult. of $\lambda_{k+1}(R_{c^\star_{k,\gamma}})$
1	$[0,1]$	$\sqrt{1+3\gamma}$	$2\pi^2\sqrt{1+3\gamma}$	1
2	$[0,\frac{4}{9}]$	$\sqrt{4+5\gamma}$	$2\pi^2\sqrt{4+5\gamma}$	1
	$[\frac{4}{9},\frac{1}{2}]$	$\sqrt{\frac{4-3\gamma}{1+3\gamma}}$	$2\pi^2\sqrt{(4-3\gamma)(1+3\gamma)}$	1
	$[\frac{1}{2},1]$	1	$5\pi^2$	2
3	$[0,\frac{35}{6\sqrt{6}}-\frac{5}{3}]$	1	$\pi^2(5+3\gamma)$	1
	$[\frac{35}{6\sqrt{6}}-\frac{5}{3},1]$	$\sqrt{\frac{8}{3}}$	$\frac{35\pi^2}{\sqrt{24}}$	2
4	$[0,\frac{19}{39}]$	$\sqrt{\frac{8}{3}}$	$\frac{\pi^2}{\sqrt{24}}(35+9\gamma)$	1
	$[\frac{19}{39},\frac{11}{15}]$	$\sqrt{\frac{9-5\gamma}{1+3\gamma}}$	$2\pi^2\sqrt{(9-5\gamma)(1+3\gamma)}$	1
	$[\frac{11}{15},1]$	$\sqrt{\frac{5}{3}}$	$\frac{32\pi^2}{\sqrt{15}}$	2
5	$[0,\frac{2\sqrt{15}\sqrt{1769}}{4065}+\frac{96}{271}]$	$\sqrt{\frac{5}{3}}$	$\pi^2(\frac{32}{\sqrt{15}}+\sqrt{15}\gamma)$	1
	$[\frac{2\sqrt{15}\sqrt{1769}}{4065}+\frac{96}{271},\frac{1}{2}]$	$\sqrt{\frac{9-8\gamma}{1+8\gamma}}$	$2\pi^2\sqrt{(9-8\gamma)(1+8\gamma)}$	1
	$[\frac{1}{2},1]$	$\{1,2\}$	$10\pi^2$	2

TABLE 2. The first four columns display k, the range of γ, the optimizers $c^\star_{k,\gamma}$, and optimal values $f^\star_{k,\gamma}$ for $k=1:5$ as defined in defined in 3.2. The fifth column gives the multiplicity of $\lambda_{k+1}(R_{c^\star_{k,\gamma}})$. See Fig. 3.2 and §3.1.

of all ellipses can be parameterized by the eccentricity. For $\epsilon\in[0,1)$, we denote by E_ϵ the ellipse of unit area with eccentricity ϵ.

The solution to the Laplace-Dirichlet eigenproblem on an ellipse is described in, e.g., [44, 45], and is briefly summarized here. In elliptical coordinates (consisting of confocal ellipse and hyperbolae), the Laplace-Dirichlet equations on an ellipse are separable. In the "angular" coordinate (parameterizing the confocal ellipses), the arising equation is called the Mathieu equation and in the "radial" coordinate (parameterizing the confocal hyperbolae), the arising equation is called the modified Mathieu equation. The eigenvalues are precisely the values for which simultaneously (1) the solution to the Mathieu equation is periodic and (2) the solution to the modified Mathieu equation vanishes on the boundary of the ellipse. To obtain the eigenvalues numerically, we use the Matlab implementation of the Mathieu equation described in [14]. Eigenvalues computed in this manner are naturally labeled $\lambda_{m,n}$ where $m=0,1,2,\dots$ are the number of zeros of the solution to the Mathieu equation and $n=1,2,\dots$ is the number of zeros of the solution to the modified Mathieu equation. We then relabel the eigenvalues λ_k for $k=1,2,\dots$ according to their magnitude. In Fig. (3.3), we plot the first 6 eigenvalues of the ellipse E_ϵ for varying eccentricity, $\epsilon\in[0,1)$. Note that as in Fig. (3.1), labeling the eigenvalues according to their magnitude introduces nondifferentiability in λ_k.

For $\epsilon\in[0,1]$, define the minimal convex combination of sequential eigenvalues over $\{E_\epsilon\colon \epsilon\in[0,1]\}$,

$$\epsilon^\star_{k,\gamma}=\arg\min_\epsilon g_{k,\gamma}(\epsilon):=(1-\gamma)\,\lambda_k(E_\epsilon)+\gamma\,\lambda_{k+1}(E_\epsilon)\quad\text{and}\quad g^\star_{k,\gamma}=g(\epsilon^\star_{k,\gamma}). \tag{3.3}$$

The optimizers $\epsilon^\star_{k,\gamma}$ and values $g^\star_{k,\gamma}$ for $k=1:5$ and $\gamma\in[0,1]$ are presented in Figs. (3.3) and (3.4). The numerical values of $g^\star_{k,\gamma}$ for $k=1:5$ and $\gamma=0:.1:1$ are given in Table 3 (middle). We observe the following:

(1) For each $k\in\mathbb{N}$ and $\gamma\in[0,1]$, the minimizer of $g_{k,\gamma}(\epsilon)$ as defined in (3.3) exists, but is not necessarily unique. Uniqueness fails for $k=2$ at $\gamma\approx 0.14$ and for $k=3$ at $\gamma\approx 0.47$.
(2) An argument similar to that for Prop. 1 shows that as a function of the parameter γ, the minimal objective function value $g^\star_{k,\gamma}$ is non-decreasing, Lipschitz continuous, and concave and that the minimizing set $\epsilon^\star_{k,\gamma}$ is upper hemicontinuous. From Fig. 3.4, we observe that the minimum $g^\star_{k,\gamma}$ is a piecewise smooth function of γ.

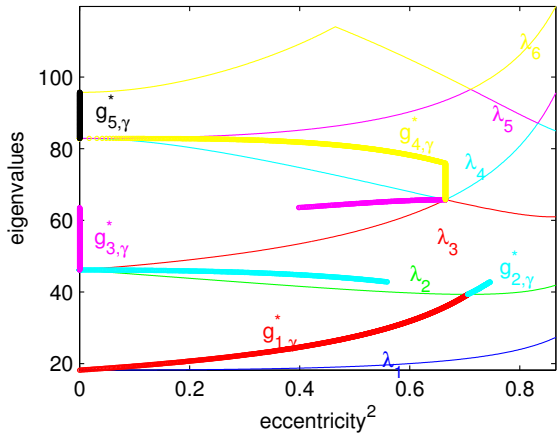

FIGURE 3.3. For $k = 1:6$, the eigenvalues λ_k of the elliptical domain E_ϵ as a function of ϵ^2. Also plotted are the optimal values $g_{k,\gamma}$ for $k = 1:5$ and $\gamma \in [0,1]$. See §3.2.

(3) For fixed $k \in \mathbb{N}$, if the optimal value $g^\star_{k,\gamma}$ is constant on the interval $[1-\delta, 1]$ for some $\delta > 0$, then $\lambda_{k+1}(E_{\epsilon^\star_{k,1}}) = \lambda_k(E_{\epsilon^\star_{k,1}})$, i.e., the multiplicity of $\lambda_{k+1}(E_{\epsilon^\star_{k,1}})$ is greater than one. This is observed for $k = 2:4$, but not $k = 5$.

4. Computational methods

In this section, we introduce a numerical approach for finding a locally optimal domain $\Omega^\star$ for an unconstrained shape optimization problem of the general form

$$\min_{\Omega \subset \mathbb{R}^d} J(|\Omega|, \Lambda(\Omega)) \tag{4.1}$$

where $\Lambda(\Omega) = \{\lambda_k(\Omega)\}_{k=1}^\infty$ is the set of Laplace-Dirichlet eigenvalues for the domain Ω. The optimization algorithm begins with an initial guess for the shape which is iteratively morphed into the optimal shape. The boundary of Ω is represented using the level set method. At each iteration, the eigenpairs of Ω are computed along with the velocity field $\mathbf{V}$, defined on $\partial\Omega$, such that $\delta J(\Omega) \cdot \mathbf{V}$ is minimal. This "velocity field of steepest descent", is continuously extended to a neighborhood of $\partial\Omega$. The boundary $\partial\Omega$ is then evolved in the direction of $\mathbf{V}$ for a distance determined by an Armijo-Wolfe line search. The process is iterated until a domain satisfying convergence criterion is attained. In what follows, we describe the eigenvalue computation and our level-set-based shape optimization approach.

Eigenvalue solver (forward problem). There are several available methods for solving eigenvalues problems on general domains, including the finite difference [30], finite element [26, 6], boundary integral [11], method of particular solutions [12, 37], and meshless methods [3]. In this paper we use the finite element method [30, 11, 26, 6].

Given a set of points on the boundary, we generate a mesh and construct the mass and stiffness matrices using linear elements. The resulting linear algebraic eigenvalue problem is solved using the Arnoldi algorithm applied to a shifted and inverted matrix [31]. The obtained eigenvalues are second-order approximations of the true eigenvalues. The generated mesh is chosen to be fine enough such that the eigenvalues have four digits of accuracy.

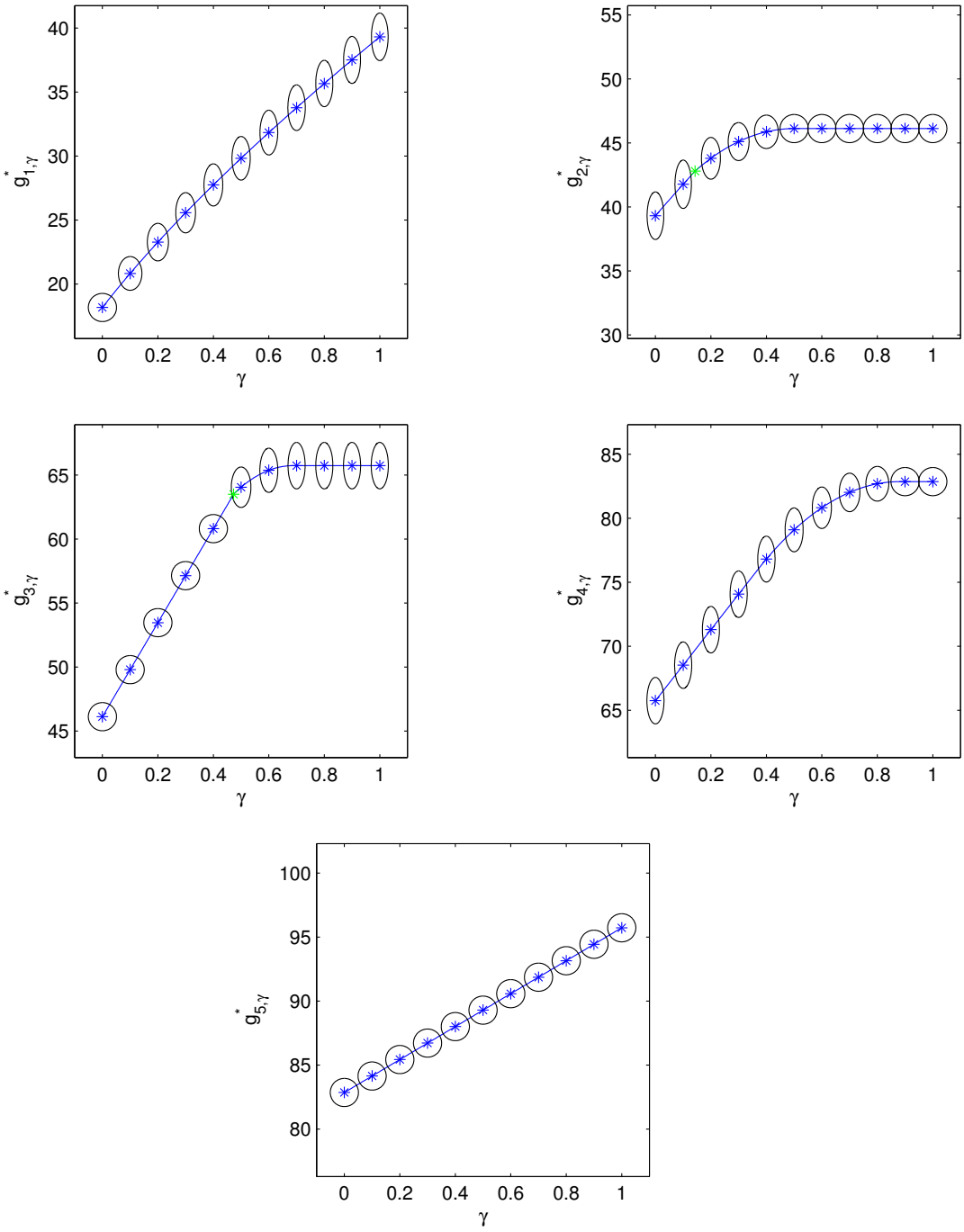

FIGURE 3.4. The optimal values $g^{\star}_{k,\gamma} = g(\epsilon^{\star}_{k,\gamma})$ for $k = 1 : 5$ and $\gamma \in [0, 1]$ as defined in (3.3) are plotted in blue. For each point indicated with an asterisk, the corresponding optimizing ellipse is also presented. See Fig. (3.3) and §3.2.

Domain representation and evolution. Recent surveys of the application of level set methods in optimal design problems are given in [9, 10] and a general reference for the level set method can be found in [36].

The level set method represents a domain $\Omega(t)$ via a function $\phi(\mathbf{x},t)\colon \mathbb{R}^d \times \mathbb{R}_+ \to \mathbb{R}$, by

$$\Omega(t) = \left\{\mathbf{x} \in \mathbb{R}^d \colon \phi(\mathbf{x},t) < 0\right\}.$$

The outward unit normal $\hat{\mathbf{n}}$ of the boundary $\partial\Omega = \phi^{-1}(0)$ can be expressed in terms of the level set function as follows:

$$\hat{\mathbf{n}} = \frac{\nabla\phi}{|\nabla\phi|}.$$

A deformation of the domain $\Omega(t)$ can be expressed as the evolution of its level set function $\phi(\cdot,t)$ by the Hamilton-Jacobi equation

$$\phi_t + V_n(\mathbf{x})|\nabla\phi| = 0 \tag{4.2}$$

where $V_n(\mathbf{x})$ is the speed of the boundary deformation.

In the solution of shape optimization problem (4.1), we seek to choose a boundary deformation speed, $V_n(\mathbf{x})$, as to reduce the value of the objective function. For objective functions of the form $J = J(|\Omega|, \Lambda(\Omega))$, the variation of J with respect to the perturbation of the boundary by a velocity field $\mathbf{V}$ is given in Proposition 2 and may be expressed as a linear functional

$$\delta J(\Omega)\cdot\mathbf{V} = \left\langle \frac{\delta J}{\delta V_n}, V_n \right\rangle_{\partial\Omega}$$

where $V_n = (\mathbf{V}\cdot\hat{\mathbf{n}})$. Thus, to first order, the boundary deformation speed $V_n(\mathbf{x})$ which most rapidly decreases the objective function value agrees with $-\frac{\delta J}{\delta V_n}$ on the boundary, i.e.

$$V_n(\mathbf{x})\Big|_{\partial\Omega} = -\frac{\delta J}{\delta V_n}.$$

To advance the level set function ϕ (and hence the domain boundary $\partial\Omega$), we must extend the boundary deformation speed to a neighborhood of $\partial\Omega$. Our method of extension differs inside and outside of the domain Ω.

(1) The linear form $\frac{\delta J}{\delta V_n}$ as stated in Prop. 2 is dependent on the magnitude of the eigenfunction gradients, which can also be evaluated on the interior of Ω. We extend $V_n(\mathbf{x})$ to the interior of Ω by simply evaluating these quantities there.
(2) On the exterior of Ω, we extend $V_n(\mathbf{x})$ by assigning to each point $\mathbf{x}$ the value $V_n(\mathbf{x_0})$ where $\mathbf{x_0} \in \partial\Omega$ is the point closest to $\mathbf{x}$. Thus, for a convex domain Ω, the velocity is constant along rays normal to $\partial\Omega$.

To compute $\frac{\delta J}{\delta V_n}$, we follow the optimize-then-discretize approach of evaluating the analytically computed variation $\frac{\delta J}{\delta V_n}$ using discrete counterparts. For this boundary deformation speed $V_n(\mathbf{x})$, the Hamilton-Jacobi equation (4.2) is solved using a 3rd-order accurate ENO scheme. If the level set function becomes either too flat or steep, we reinitialize the level set function to a signed distance function to the boundary $\partial\Omega$, again using a 3rd-order accurate ENO scheme.

Once a deformation speed $V_n(x)$ has been chosen, the level set is evolved according to the Hamilton Jacobi equation (4.2) for a time t which satisfies the Armijo-Wolfe conditions which guarantees a reduction in the objective function value and slope [35]. The process is continued until convergence criteria are met.

In the level set representation of the domain Ω, the boundary $\partial\Omega = \phi^{-1}(0)$ is only defined implicitly. At each iteration, points on the boundary may be approximated from the local representation of $\phi(\mathbf{x})$ on the mesh. We use the second order approximation of the boundary as described in [13]. Note that only the quadratic polynomial for each cell interface must be constructed; it is not necessary to construct the bicubic polynomial on each cell.

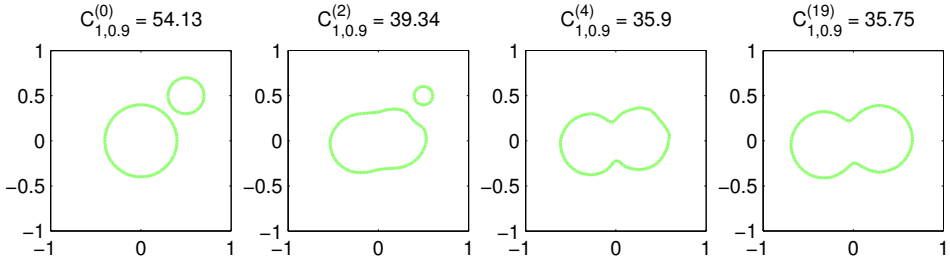

FIGURE 5.1. The evolution of the domain represented by a level set function for the optimization of $C_{1,0.9}$. The shapes for the 0-th, 2-nd, 4-th, and 19-th iterations are shown. See §5.

5. Convex combinations of sequential Laplace-Dirichlet eigenvalues

In this section, we apply the computational method developed in §4 to study the convex combination of sequential Laplace-Dirichlet eigenvalues. Define, for fixed $k \in \mathbb{N}$ and $\gamma \in [0,1]$, the γ-parameterized shape optimization problem

$$\Omega^\star_{k,\gamma} = \arg\min_{\Omega} C_{k,\gamma}(\Omega) := (1-\gamma)\,|\Omega|\,\lambda_k(\Omega) + \gamma\,|\Omega|\,\lambda_{k+1}(\Omega) \quad \text{and} \quad C^\star_{k,\gamma} = C_{k,\gamma}(\Omega^\star_{k,\gamma}). \tag{5.1}$$

Using Prop. 3, we choose the boundary deformation speed for this objective function to be

$$C(x)|_{\partial\Omega} = |\Omega|\left((1-\gamma)\,|\partial_n\psi_k|^2 + \gamma\,|\partial_n\psi_{k+1}|^2\right) - ((1-\gamma)\lambda_k + \gamma\lambda_{k+1}) \tag{5.2}$$

where $\|\psi_k\|_{L^2(\Omega)} = \|\psi_{k+1}\|_{L^2(\Omega)} = 1$. The algorithm starts with an initial guess of the domain represented by a level set function, $\phi(\mathbf{x})$, on a 64×64 rectangular grid. To create a mesh for the finite element computation of the eigenvalues, points on the zero level set contour are approximately found using a second order approximation of the boundary [13]. The mesh is created by the built-in Matlab function "initmesh" which uses a Delaunay triangulation algorithm with default parameters and maximum edge size is chosen as 0.5 times the rectangular grid size. The finite element discretization of (2.1) for a given shape Ω is solved to obtain eigenpairs $\{\lambda_j, \psi_j\}_{j=1}^{k+1}$. The deformation speed (5.2) is then calculated on the triangulated mesh of Ω. We interpolate the deformation speed to the rectangular grid using a linear interpolation and extend it to the exterior of Ω using the closest point method. The level set function is then advected by this deformation speed using a linesearch algorithm, allowing for large step sizes. This process is repeated until the difference of objective function values at subsequent iterations is less than 10^{-2}.

We first demonstrate the flexibility of the level set approach to topological changes in the domain. In Figure 5.1, we optimize $C_{k,\gamma}$ for $k = 1$ and $\gamma = 0.9$ with the initial guess given by two disjoint balls, represented by the zero level set of function

$$\phi(x,y) = \min\left\{\sqrt{(x-0.5)^2+(y-0.5)^2} - 0.2, \sqrt{x^2+y^2} - 0.4\right\}.$$

During the optimization process, the small ball diminishes and finally disappears while the larger ball grows and deforms into the optimal shape, which looks like two slightly overlapping balls. The domains for the 0-th, 2-nd, 4-th, and 19-th iterations are given in Figure 5.1. Since the topology of the optimal shape is unknown in advance, it is advantageous to use the level set method, which automatically handles changes in the topology.

Furthermore, in Figure 5.2, we optimize $C_{k,\gamma}$ for $k = 1$ and $\gamma = 1$ using for an initial guess the union of two slightly overlapping balls, represented as the zero level set of the function

$$\phi(x,y) = \min\left\{\sqrt{(x-0.2)^2+(y-0.2)^2} - 0.32, \sqrt{(x+0.2)^2+(y+0.2)^2} - 0.32\right\}.$$

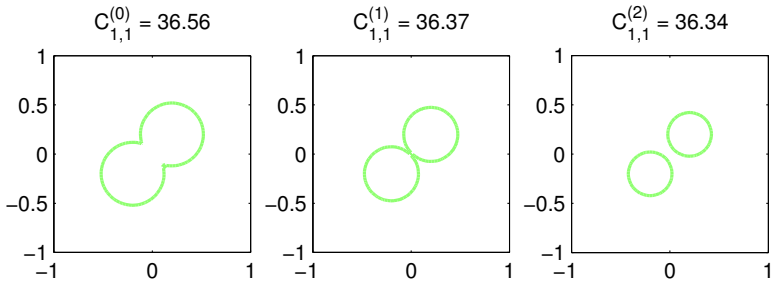

FIGURE 5.2. The evolution of the shape represented by a level set function during the optimization of $C_{1,1}$. The shape at the 0-th, 1-st, and 2-nd iterations are shown. See §5.

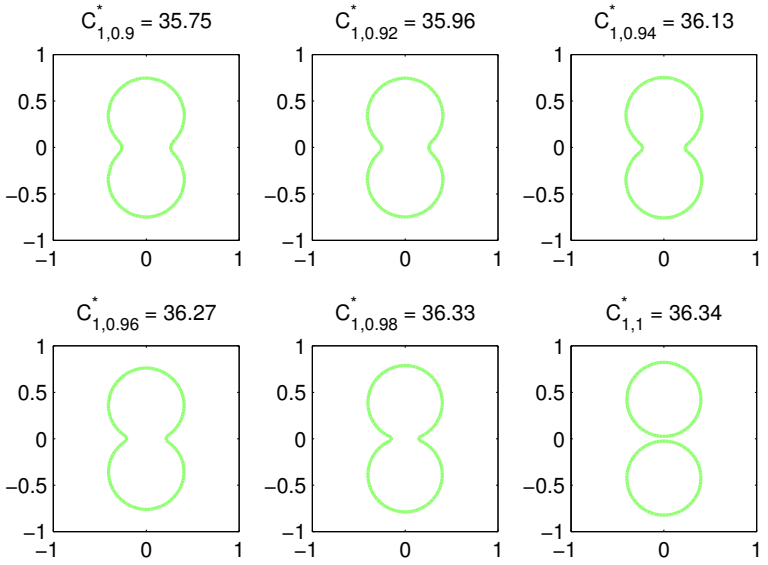

FIGURE 5.3. The optimal shapes for $C^*_{1,\gamma}$ for γ ranging from 0.9 to 1 with increment 0.02. See §5.

During the optimization iterates, the shape deforms into two disconnected balls of equal size. The domains for the initial, first, and second iterations are given in Figure 5.2. By the second iteration, the domain has already converged to the analytically known optimal shape.

Another advantage of the level set method is the generality of domains which may be represented. For a Fourier representation of the boundary, the domains which may be represented are restricted to star shaped domains with smooth boundary. In Figure 5.3, we plot $\Omega^\star_{k,\gamma}$ for γ ranging from 0.9 to 1 with increment 0.02. Our method accurately captures the optimal shape as it becomes disconnected when $\gamma \uparrow 1$.

Similar to other local methods, gradient-based level set methods may reach a local minimum instead of a global minimum. However, due the flexibility of topological changes, the level set approach is more robust in providing the global minimum than other approaches.

$\gamma\backslash k$	1	2	3	4	5
0	19.74	39.48	49.35	70.51	81.55
0.1	22.51	41.87	52.31	72.33	85.37
0.2	24.97	44.14	55.27	74.14	89.19
0.3	27.21	46.29	58.23	75.95	93.01
0.4	29.28	48.35	61.19	77.76	96.84
0.5	31.21	49.35	64.15	79.57	98.70
0.6	33.03	49.35	67.11	80.91	98.70
0.7	34.75	49.35	70.07	81.51	98.70
0.8	36.40	49.35	70.51	81.55	98.70
0.9	37.97	49.35	70.51	81.55	98.70
1.0	39.48	49.35	70.51	81.55	98.70

$\gamma\backslash k$	1	2	3	4	5
0	$18.17 = \pi j_{0,1}^2$	39.32	$46.12 = \pi j_{1,1}^2$	65.74	$82.86 = \pi j_{2,1}^2$
0.1	20.83	41.77	49.80	68.52	84.15
0.2	23.28	43.80	53.47	71.29	85.43
0.3	25.57	45.11	57.15	74.06	86.72
0.4	27.74	45.87	60.82	76.81	88.01
0.5	29.83	46.12	64.05	79.09	89.29
0.6	31.83	46.12	65.38	80.82	90.58
0.7	33.78	46.12	65.74	82.01	91.87
0.8	35.67	46.12	65.74	82.69	93.15
0.9	37.51	46.12	65.74	82.86	94.44
1.0	39.32	$46.12 = \pi j_{1,1}^2$	65.74	$82.86 = \pi j_{2,1}^2$	$95.73 = \pi j_{0,2}^2$

$\gamma\backslash k$	1	2	3	4	5
0	$18.17 = \pi j_{0,1}^2$	$36.34 = 2\pi j_{0,1}^2$	$46.12 = \pi j_{1,1}^2$	64.29	78.19
0.1	20.83	39.43	49.70	68.36	82.58
0.2	23.27	43.64	53.08	71.13	85.43
0.3	25.53	45.08	56.31	73.36	86.72
0.4	27.64	45.87	59.41	75.08	88.01
0.5	29.60	46.12	62.34	76.42	88.52
0.6	31.42	46.12	64.29	77.56	88.52
0.7	33.08	46.12	64.29	78.18	88.52
0.8	34.56	46.12	64.29	78.19	88.52
0.9	35.75	46.12	64.29	78.19	88.52
1.0	$36.34 = 2\pi j_{0,1}^2$	$46.12 = \pi j_{1,1}^2$	64.29	78.19	88.52

TABLE 3. Values of $f_{k,\gamma}^\star$ as defined in (3.2) (top), $g_{k,\gamma}^\star$ as defined in (3.3) (middle), and $C_{k,\gamma}^\star$ as defined in (5.1) (bottom) for $k = 1 : 5$ and $\gamma = 0 : .1 : 1$. The optimizers are plotted in Figs. 3.2, 3.4, and 5.4. See §3.1, §3.2, and §5.

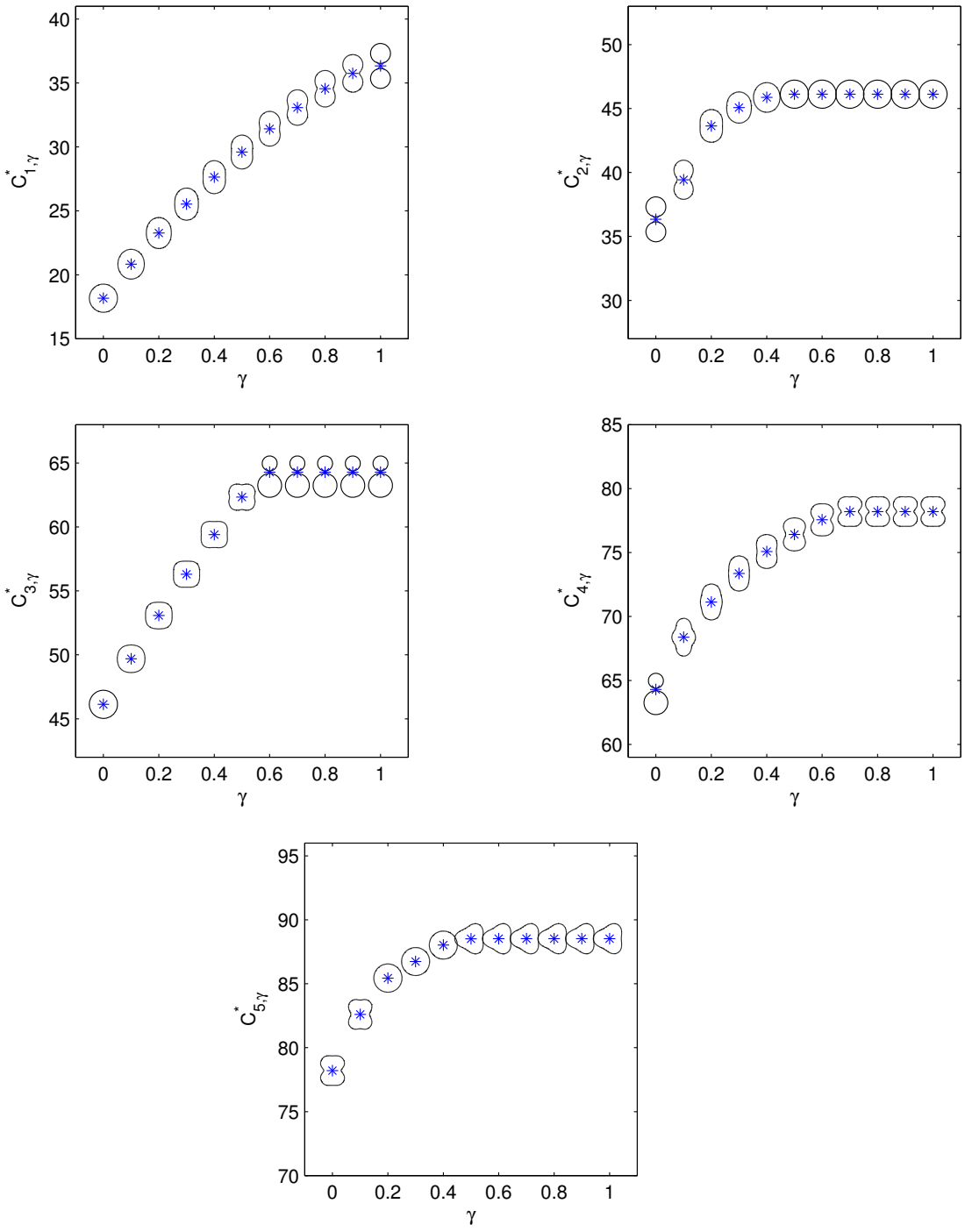

FIGURE 5.4. Plots of $C^\star_{k,\gamma}$ (blue asterisks) and the minimizers $\Omega^\star_{k,\gamma}$ for $k = 1:5$ and $\gamma = 0:.1:1$. See §5 and Table 3.

We numerically solve (5.1) for $k = 1:5$ and $\gamma = 0:.1:1$. The results are summarized in Table 3 (bottom) and Fig. 5.4. The results may be compared to those in §3, where the optimal values for restricted class of domains (rectangles and ellipses) were investigated. We observe the following:

(1) By Prop. 1, for each $k \in \mathbb{N}$ and $\gamma \in [0,1]$, the minimizer of $C_{k,\gamma}(\Omega)$ as defined in (5.1) exists, but is not necessarily unique. For example, for $k = 3$, there exists a $\gamma_c \in [0.5, 0.6]$ such that there are two minimizers. At $\gamma = \gamma_c$ the minimizer is not lower hemicontinuous.
(2) Proposition 1 shows that as a function of the parameter γ, the minimal objective function value $C^\star_{k,\gamma}$ is non-decreasing, Lipschitz continuous, and concave and that the minimizing set $\Omega^\star_{k,\gamma}$ is upper hemicontinuous.
(3) For fixed $k \in \mathbb{N}$, if the optimal value $C^\star_{k,\gamma}$ is constant on the interval $[1-\delta, 1]$ for some $\delta > 0$, then $\lambda_{k+1}(\Omega^\star_{k,1}) = \lambda_k(\Omega^\star_{k,1})$, i.e., the multiplicity of $\lambda_{k+1}(\Omega^\star_{k,1})$ is greater than one. This is observed for $k = 2:5$.
(4) For the values of k and γ considered, the minimizing domain has at least one axis of symmetry. Note that this property fails for $k = 13$ and $\gamma = 0$ [3].
(5) For $k = 1:5$ and $\gamma = 1$, our numerical results agree with [40, 3] and for $k = 1:5$ and $\gamma = 0.5$, our numerical results agree with [2].
(6) The optimal values obtained for domains which can be represented by a level-set function are at least as small as those obtained for rectangles and ellipses; see Table 3. For several parameter values, the objective function values and minimizers are similar. For example, for $k = 5$ and $\gamma = 0.3$, the optimal shape is a nearly a ball and for $k = 3$ and $\gamma = 0.4$, the optimal shape resembles a square with rounded corners.
(7) For $k = 1$, we observe that the family of optimal solutions $\Omega^\star_{1,\gamma}$ for $\gamma \in [0,1]$ is a deformation between $\Omega^\star_{1,0}$ (= ball) and $\Omega^\star_{1,1}$ (= union of two balls of equal size). It is known that $\Omega^\star_{1,\gamma}$ is disconnected only for $\gamma = 1$ [46, 25], as illustrated in Fig. (5.3). Furthermore, our numerical studies support the conjecture that for $\gamma \in [0,1)$, $\Omega^\star_{1,\gamma}$ has two axes of symmetry and is simply connected (c.f. [46] and [22, open problem 21]). The value γ for which $\Omega^\star_{1,\gamma}$ is no longer convex is $\gamma_c \approx 0.36$.
(8) Our numerical results support the conjecture that the disk minimizes $C_{k,\gamma}$ for $k = 2$ and $\gamma = \frac{1}{2}$ [22, open problem 17]. We show below in Prop. 4 that the disk is a local minimizer for $\gamma \in [\frac{1}{2}, 1]$.

Proposition 4. *The disk is a local minimizer of $C_{2,\gamma}(\Omega)$ for $\gamma \in [\frac{1}{2}, 1]$.*

Proof. Our proof is only a slight modification to the proof that the disk is a local minimum of $\lambda_3(\Omega)$ given in [46, Thm. 8.3], to which we refer the reader for details. Consider the nearly circular domain $\Omega_\epsilon = \{(r,\theta) : r < R(\theta,\epsilon),\ \theta \in [0, 2\pi]\}$ where

$$R(\theta,\epsilon) := 1 + \epsilon \sum_{n=-\infty}^{\infty} a_n e^{in\theta} + \epsilon^2 \sum_{n=-\infty}^{\infty} b_n e^{in\theta} + \mathcal{O}(\epsilon^3), \quad a_n = \overline{a_{-n}} \text{ and } b_n = \overline{b_{-n}}.$$

Using the asymptotic formulas for $|\Omega_\epsilon|\lambda_k(\Omega_\epsilon)$ given in [46, App. A], the following holds. If $a_2 \neq 0$,

$$C_{2,\gamma}(\Omega_\epsilon) = \pi j_{1,1}^2 \left[1 + 2(2\gamma - 1)|\epsilon||a_2|\right] + \mathcal{O}(\epsilon^2)$$

and if $a_2 = 0$,

$$C_{2,\gamma}(\Omega_\epsilon) = \pi j_{1,1}^2 + A\epsilon^2 + (1 - 2\gamma)B\epsilon^2 + \mathcal{O}(\epsilon^3)$$

where B is a non-negative constant, dependent on $\{a_n\}$ and b_2 and A is a non-negative constant, dependent on $\{a_n\}$, which vanishes only if $a_n = 0$ for all n. In both cases, if $\gamma \in [\frac{1}{2}, 1]$, any perturbation of the disk increases $C_{2,\gamma}$, showing that the disk is a local minimum. □

6. Discussion and further directions

We have presented a general method for computing (local) minima of shape optimization problems where the objective function is dependent on the Laplace-Dirichlet eigenvalues of the shape. The numerical method utilizes the level-set method for describing the shape of the domain and is thus suitable for studying shape optimization problems where the topology of the minimizer is unknown.

The method is applied to the problem of minimizing the convex combination of sequential eigenvalues, $C_{k,\gamma}(\Omega) = (1-\gamma)\lambda_k(\Omega) + \gamma\lambda_{k+1}(\Omega)$. It is known that for some values of k, the number of connected components of the minimizer for this parameterized objective function varies with the convex combination parameter, γ. This feature makes this problem an excellent application for our method. We are able to show that the minimal value of $C_{k,\gamma}$ is a non-decreasing, Lipschitz continuous, and concave function of γ and that the minimizing set is upper hemicontinuous in γ. Numerically, we are able to reproduce several known results for appropriate parameter values and also computationally address several open problems within the community. In particular, we observe that for $k = 2, 3, 4, 5$, if $\Omega^\star$ is the optimizer for $\gamma = 1$, then $\Omega^\star$ is also an optimizer on an interval $\gamma \in [1-\delta, 1]$ for some $\delta > 0$ and that $C^\star_{k,\gamma}$ is constant. Consequently, for these values of k and γ, the k-th and $k+1$-th eigenvalues of the minimizer are equal, i.e., $\lambda_k(\Omega^\star_{k,\gamma}) = \lambda_{k+1}(\Omega^\star_{k,\gamma})$. Our general results are also compared to results obtained for rectangles and ellipses (see §3).

There are several interesting extensions of this work. For the computation of eigenvalues, we used a finite element method, which is robust, but does not have the accuracy of boundary integral or meshless methods. We view the merging of one of these methods with the level set method for the representation of the domain as a challenging but natural extension of this work. There are also several ways in which our finite element implementation could be improved. For instance, at each iteration, we use a rootfinding algorithm to find approximate points on the boundary and remesh the domain. This could be improved by reusing mesh information from the previous iterations. Finally, the methods developed here can be used to study a large number of eigenvalue optimization problems. One particular extension would be to consider convex combinations of three eigenvalues, such as studied in [25].

Acknowledgements. Braxton Osting is supported in part by a National Science Foundation (NSF) Postdoctoral Fellowship DMS-11-03959. Chiu-Yen Kao is supported in part by a Northrop Grumman Corporation Grant. We thank Dorin Bucur and Antoine Henrot for useful discussions.

References

[1] V. Akcelik, G. Biros, O. Ghattas, D. Keyes, K. Ko, L.-Q. Lee, and E. G. Ng. Adjoint methods for electromagnetic shape optimization of the low-loss cavity for the international linear collider. *J. Phys: Conference Series*, 16:435–445, 2005.

[2] P. R. S. Antunes. Optimization of sums and quotients of Dirichlet-Laplacian eigenvalues. *Applied Mathematics and Computation*, 2012. preprint.

[3] P. R.S. Antunes and P. Freitas. Numerical optimization of low eigenvalues of the Dirichlet and Neumann Laplacians. *Journal of Optimization Theory and Applications, in press*, 2012.

[4] M. S. Ashbaugh and R. D. Benguria. Isoperimetric inequalities for eigenvalues of the Laplacian. *Proc. of Symposia in Pure Math.*, 76(1):105–139, 2007.

[5] M.S. Ashbaugh and R. Benguria. A sharp bound for the ratio of the first two eigenvalues of Dirichlet Laplacians and extensions. *Ann. of Math.*, 135:601–628, 1992.

[6] D. Boffi. Finite element approximation of eigenvalue problems. *Acta Numerica*, 19(-1):1–120, 2010.

[7] D. Bucur. Minimization of the k-th eigenvalue of the Dirichlet Laplacian. preprint, 2011.

[8] D. Bucur and G. Buttazzo. *Variational Methods in Shape Optimization Problems*. Birkhäuser, 2005.

[9] M. Burger. A framework for the construction of level set methods for shape optimization and reconstruction. *Inverse Problems*, 17:1327–1356, 2001.

[10] M. Burger and S. J. Osher. A survey on level set methods for inverse problems and optimal design. *European Journal of Applied Mathematics*, 16:263–301, 2005.

[11] G. Chen and J. Zhou. *Boundary Element Methods*. Academic Press Publications, London, 1992.

[12] J.T. Chen, I.L. Chen, and Lee. Eigensolutions of multiply connected membranes using the method of fundamental solutions. *Engineering Analysis with Boundary Elements*, pages 166–174, 2005.

[13] D. L. Chopp. Some improvements of the fast marching method. *SIAM J. Sci. Comput.*, 23(1):230–244, 2001.
[14] E. Cojocaru. Mathieu functions computational toolbox implemented in Matlab. *ArXiv e-prints*, 2008.
[15] R. Courant and D. Hilbert. *Methods of mathematical physics. Vol. I.* Interscience Publishers, Inc., New York, N.Y., 1953.
[16] S. Cox. The two phase drum with the deepest bass note. *Japan J. Indust. Appl. Math.*, 8:345–355, 1991.
[17] S. Cox and J. McLaughlin. Extremal eigenvalue problems for composite membranes, i and ii. *Applied Math. And Optimization*, 22:153–167 and 169–187, 1990.
[18] S. J. Cox and D. C. Dobson. Maximizing band gaps in two-dimensional photonic crystals. *SIAM J. Appl. Math.*, 59:2108–2120, 1999.
[19] S. J. Cox and D. C. Dobson. Band structure optimization of two-dimensional photonic crystals in H-polarization. *J. Comput. Phys.*, 158:214–224, 2000.
[20] P. Grinfeld. Hadamard's formula inside and out. *J. Optim. Theory Appl.*, 145, 2010.
[21] Lin He, Chiu-Yen Kao, and Stanley Osher. Incorporating topological derivatives into shape derivatives based level set methods. *Journal of Computational Physics*, 225(1):891 – 909, 2007.
[22] A. Henrot. *Extremum Problems for Eigenvalues of Elliptic Operators*. Birkhäuser Verlag, 2006.
[23] D. Henry. *Perturbation of the Boundary in Boundary-Value Problems of Partial Differential Equations*. Cambridge University Press, 2005.
[24] M. Hintermüller, C. Y. Kao, A. Laurain, M. Hintermüller, C. Y. Kao, and A. Laurain. Principal eigenvalue minimization for an elliptic problem with indefinite weight and robin boundary conditions. *Applied Mathematics & Optimization*, pages 1–36, December 2011.
[25] M. Iversen and D. Mazzoleni. Minimizing convex combinations of low eigenvalues. 2012.
[26] C. Johnson. *Numerical solution of partial differential equations by the finite element method*. Lund,Sweden, 1987.
[27] C.-Y. Kao, Y. Lou, and E. Yanagida. Principal eigenvalue for an elliptic problem with indefinite weight on cylindrical domains. *Mathematical Biosciences and Engineering*, 5:315–335, 2008.
[28] C. Y. Kao, S. Osher, and E. Yablonovitch. Maximizing band gaps in two dimensional photonic crystals by using level set methods. *Applied Physics B: Lasers and Optics*, 81:235–244, 2005.
[29] J. R. Kuttler and V. G. Sigillito. Eigenvalues of the Laplacian in two dimensions. *SIAM Review*, 26(2):163–193, 1984.
[30] S. Larsson and V. Thomée. *Partial Differential Equations with Numerical Methods*. Springer-Verlag, New York, 2005.
[31] R.B. Lehoucq, D.C. Sorensen, and C. Yang. *ARPACK Users' Guide: Solution of large-scale eigenvalue problems with implicitly restarted Arnoldi methods*.
[32] M. Levitin and R. Yagudin. Range of the first three eigenvalues of the planar Dirichlet Laplacian. *LMS J. Comput. Math.*, 6:1–17, 2003.
[33] N.D. Manh, A. Evgrafov, A.R. Gersborg, and J. Gravesen. Isogeometric shape optimization of vibrating membranes. *Computer Methods in Applied Mechanics and Engineering*, pages 1343–1353, 2011.
[34] D. Mazzoleni and A. Pratelli. Existence of minimizers for spectral problems. preprint CVGMT, 2011.
[35] J. Nocedal and S. Wright. *Numerical Optimization*. Springer, second edition, 2006.
[36] Stanley J. Osher and Ronald P. Fedkiw. *Level Set Methods and Dynamic Implicit Surfaces*. Springer, 1 edition, 2002.
[37] B. Osting. Optimization of spectral functions of Dirichlet-Laplacian eigenvalues. *J. Comp. Phys.*, 229(22):8578–8590, 2010.
[38] B. Osting. Bragg structure and the first spectral gap. *Appl. Math. Lett.*, 2012. doi:10.1016/j.aml.2012.03.002.
[39] B. Osting and M. I. Weinstein. Long-lived scattering resonances and Bragg structures. submitted, 2011.
[40] E. Oudet. Numerical minimization of eigenmodes of a membrane with respect to the domain. *ESAIM: Control, Optimization and Calculus of Variations*, 10:315–335, 2004.
[41] L.E. Payne, G. Pólya, and H.F. Weinberger. On the ratio of consecutive eigenvalues. *J. Math. Phys.*, 35:289–298, 1956.
[42] John William Strutt Rayleigh. *The Theory of Sound*, volume 1. Macmillan and co., 1877.
[43] Yu-Chen Shu, Chiu-Yen Kao, I-Liang Chern, and Chien C. Chang. Augmented coupling interface method for solving eigenvalue problems with sign-changed coefficients. *J. Comput. Phys.*, 229(24):9246–9268, December 2010.
[44] B. Andreas Troesch. Elliptical membranes with smallest second eigenvalue. *Mathematics of Computation*, pages 767–772, 1973.
[45] B. Andreas Troesch and H. R. Troesch. Eigenfrequencies of an elliptic membrane. *Mathematics of Computation*, pages 755–765, 1973.
[46] S. A. Wolf and J. B. Keller. Range of the first two eigenvalues of the Laplacian. *Proc. R. Soc. Lond. A*, 447:397–412, 1994.

E-mail address: braxton@math.ucla.edu, kao@math.ohio-state.edu.

Osting: Department of Mathematics, University of California, Los Angeles, CA 90095, Kao: Address1: Department of Mathematics, The Ohio State University, Columbus, OH 43210, USA; Address 2: Department of Mathematics and Computer Science, Claremont McKenna College, CA 91711.